Winter Weather On Mars: The Unique Southern Hemsiphere. J. R. Barnes and D. Tyler, College of Oceanic and Atmospheric Sciences, 104 COAS Admin. Bldg., Oregon State University, Corvallis, OR, 97331, barnes@oce.orst.edu, dtyler@oce.orst.edu.

Introduction: The Mars Global Surveyor Mission has allowed a characterization of many of the basic aspects of winter weather on Mars. In particular, the TES temperature data, along with RS data, have been analyzed to show that traveling weather systems (transient eddies) are prominent in both hemispheres outside of the summer season [1,2,11]. Those in the northern hemisphere are typically significantly stronger than those in the southern hemisphere, as first predicted on the basis of Mars GCM experiments [3]. The northern weather systems were first observed in-situ by the Viking Meteorology Experiment [4,5]. Under relatively dusty conditions, not overly far away from solstice, the northern disturbances become very strongly upper-level in character, exhibiting maximum amplitudes at heights of ~25 km and above. These upper-level disturbances were also almost certainly observed – indirectly, via the smallness of their surface amplitudes – by Viking during the solstice dust storm of 1977 [4].

The weather systems in the southern hemisphere, as revealed for the first time by the MGS data, are very different in a number of basic respects from those in the north. The very large-amplitude and strongly upper-level disturbances (which are very slowly propagating) have not been observed in the south. The southern systems are generally characterized by shallower vertical structures, and somewhat shorter zonal scales than the northern systems. They also tend to have somewhat shorter time scales (periods). The southern disturbances are quite weak in the seasonal period around solstice, but they become much more intense in mid-winter (starting around L_s~130-135).

In both hemispheres, the weather system activity tends to be much stronger in certain longitudinal regions, the storm zones. The existence of these was first predicted on the basis of GCM studies [6]. In the north, the storm zones tend to coincide with the major lowland regions of Acidalia and Utopia/Arcadia [1]. These storm zones extend to upper-levels when the disturbances have their maximum amplitudes in this part of the atmosphere. In the lowland regions, the storms often penetrate well to the south during the seasonal periods when their amplitudes are largest at lower levels. When they do so they frequently are associated with local dust storm activity, and this activity can then move across the equator into the southern hemisphere [7,8].

The southern hemisphere storm zone structure is dramatically different than that in the north [1]. In particular, there is really only one basic region of enhanced activity. This is a region which extends from areas southward of the extension of the Tharsis plateau eastward to the vicinity of the Argyre basin. More broadly, the western hemisphere exhibits much stronger storm activity in the south than the eastern hemisphere does. The western hemisphere is also substantially colder on average than the eastern hemisphere, at a given latitude. The combination of these two pronounced east-west hemispheric asymmetries appears to play a very important role in the location of the south polar residual cap and the cryptic region [9].

In this paper we will summarize some of the key observational aspects of the southern hemisphere winter weather. Modeling studies have recently enabled some important insights to be gained into the unique dynamics of the southern hemisphere winter circulation, which is influenced to a remarkable extent by the enormous topography associated with the Hellas basin, as well as that associated with Tharsis and Argyre.

Observations: Fig. 1 shows the seasonal variation in the weather activity in the TES temperature data during the first and the third MGS mapping years. It can be seen that the amplitude of the disturbances is greatest during middle and late winter, and is quite small during a period around the winter solstice. There is a secondary maximum in the amplitudes during the autumn season, L_s~30-60. In the second mapping year (not shown) the seasonal variation is very similar, up until the occurrence of the global dust storm shortly after L_s~180. This storm dramatically altered the thermal structure in the south and gave rise to stronger activity at upper levels (than seen in the first and third years).

The seasonal variation in the southern winter weather activity is particularly interesting in relation to Mars Odyssey observations of polar Argon abundances. Analyses of these have shown that the north-south transport of Argon by eddies increases greatly in the mid-winter period, limiting the rise of Argon enhancements in the south polar region [10]. The analyses indicate that this north-south mixing by eddies remains strong well into southern spring. The TES data show the weather systems decreasing sharply in strength after the early spring, but it is possible that the systems become so shallow in structure that TES is not able to see them. Alternatively, other types of eddies

(quasi-stationary and thermal tides) may be critical for the Argon transports later in the spring season.

Throughout the winter period, the weather activity in the south varies quite strongly in longitude at lower atmospheric levels. This is illustrated in Fig. 2, which shows the average variance of the disturbances versus longitude and latitude at a lower level (~ 3.7 mb), for the L_s~136-155 and the L_s~183-201 seasonal periods in the first mapping year. The activity can be seen to be strongest in the ~ 210-300 E region in the first case, which corresponds to the area of the southward extension of Tharsis extending eastward to the Argyre basin. In the early spring case, the activity is strongest in the eastern part of this region. Similar patterns characterize the lower-level weather activity throughout southern winter, in all three of the TES mapping years: in general, the activity is much stronger in the western hemisphere than in the eastern one. At upper levels, however, the patterns can be quite different, with typically less zonal asymmetry than at lower levels.

An average picture of the synoptic structure of the TES weather disturbances, for the L_s~136-155 mid-winter period in the first mapping year, is shown in Fig. 3. This is a single-point correlation map computed using twice-daily synoptic maps generated using the FFSM method [1]. It can be seen that the disturbances are certainly the most highly coherent within the storm zone region, but they do possess a global coherence. The structure in the storm zone is very consistent with that of a front, within the limitations of the TES longitudinal resolution. Zonal wavenumbers 1-4 all have sizeable amplitudes, producing the relatively confined storm zone in Fig. 2. The dominant modes share a well-defined period of ~ 2.0-2.3 sols. The structure of the wavenumber 4 mode, which has the largest amplitude, is shown in Fig. 4. It can be seen that this mode has a relatively shallow structure in the vertical.

Analyses of MGS RS data have revealed the southern weather systems, and have allowed a determination of the low-level geopotential height perturbations and estimates of the low-level meridional winds [11]. These are fairly large in the mid-winter period, with amplitudes of ~200 meters and ~10-15 m/s in the western hemisphere storm zone. One important aspect of the southern winter weather systems in both the MGS TES and RS data is that temperatures in the cold sectors often fall below the CO_2 frost point [9,11].

A very prominent component of the southern winter circulation, as revealed by the TES and RS data [12], is a large-amplitude quasi-stationary wave pattern. At lower levels this pattern can have a fairly strong wave 2 character, but at upper levels it is dominated by wave 1, as in Fig. 5. The western hemisphere tends to be relatively cold, while the eastern hemisphere is warm. The warmest region is essentially centered on Hellas at upper levels. The RS data show that at low levels there is a time-mean low pressure center in the vicinity of Hellas, as well as one near Argyre; there is a ridge in the vicinity of Tharsis [12].

Modeling and Dynamics: GCM simulations have been at least fairly successful in simulating the weaker nature of the weather activity in southern winter as compared to northern winter (it was on the basis of these that this basic asymmetry was first predicted [3]). Controlled studies have shown that the north-south weather asymmetry is associated with both the topography and the seasonal asymmetry in thermal forcing for Mars [3]. It is not clear that the GCM's presently provide a good simulation of the variation in the weather activity during southern winter – in particular, the intensification in this activity during middle and late winter (and perhaps the spring as well). The extent to which GCM simulations reproduce the observed storm zone structure in the south is also unclear at present, as are the basic dynamics underlying this storm zone. Lee cyclogenesis associated with the southward extension of Tharsis may be important for the latter, as may the time-mean circulation in the vicinity of Hellas.

Recent relatively high-resolution simulations with the OSU Mars Mesoscale Model (running with a semi-global domain) for the L_s~120 season have yielded a storm zone structure which is in quite good agreement with the TES data. Fig. 6 shows the model storm zone pattern in the surface pressure field. One potentially important aspect of this simulation is that the TES-observed seasonal polar cap boundary has been specified in the model. Another is that the specified fixed dust loading has been adjusted somewhat to yield relatively good agreement between the simulated and observed zonal-mean thermal fields. As has previously been found in NASA Ames GCM simulations (Hollingsworth, personal communication), a very strong vortex-like time-mean circulation is present in the vicinity of Hellas. A weaker such circulation is present near Argyre. The Hellas and Argyre circulations are cyclonic at lower levels, as can be seen in Fig. 7. The Hellas circulation is strongly warm-core, as in the TES data (see Fig. 5).

New results from currently on-going analyses of the mesoscale model simulations will be presented and discussed, particularly as they relate to the storm zone structure and dynamics. It is expected that considerable insight into the basic dynamics of the unique southern winter weather regime can be gained from these model studies in conjunction with the MGS TES and RS data.

References: [1] Barnes, J.R. (2003) *Sixth International Conference on Mars*, Abstract #3127. [2] Banfield, D.B., Conrath, B.J., Gierasch, P.J., Wilson, R.J., and Smith, M.D. (2004) *Icarus, 170*, 365-403. [3] Barnes, J.R., Pollack, J.B., Haberle, R.M., Zurek, R.W., Leovy, C.B., Lee, H., and Schaeffer, J. (1993) *J. Geophys. Res., 98*, 3125-3148. [4] Barnes, J.R. (1980) *J. Atmos. Sci., 37*, 2002-2015. [5] Barnes, J.R. (1981) *J. Atmos. Sci., 38*, 225-234. [6] Hollingsworth, J.L., Haberle, R.M., Barnes, J.R., Bridger, A.F.C., Pollack, J.B., Lee, H., and Schaeffer, J. (1996) *Nature, 380*, 413-416. [7] Wang, H., Richardson, M.I., Wilson, R.J., Ingersoll, A.P., Toigo, A.D., and Zurek, R.W. (2003) *Geophys. Res. Lett., 30(9)*, 1488. [8] Wang, H., Zurek, R.W., and Richardson, M.I. (2005) *J. Geophys. Res., 110*, doi:10.1029/2005JE002423. [9] Colaprete, A., Barnes, J.R., Haberle, R.M., Hollingsworth, J.L., Kieffer, H.H., and Titus, T.N. (2005) *Nature, 435*, 10.1038. [10] Sprague, A.L., Boynton, W.V., Kerry, K.E., Janes, D.N., Hunten, D.M., Kim, K.J., Reedy, R.C., and Metzger, A.E. (2004) *Science, 306*, 1364-1367. [11] Hinson, D.P., and Wilson, R.J. (2002) *Geophys. Res. Lett., 29(7)*, doi: 10.1029/2001GL014103. [12] Hinson, D.P., Wilson, R.J., Smith, M.D., and Conrath, B.J. (2003) *J. Geophys. Res., 108*, 5004.

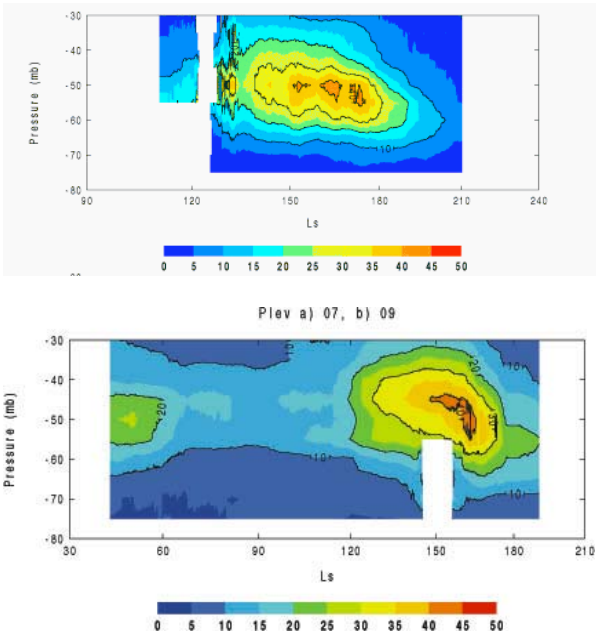

Fig. 1: Variation of the weather activity (variance) in the TES temperature data at the 3.7 mb level during southern winter, for the first (top) and third (bottom) MGS mapping years.

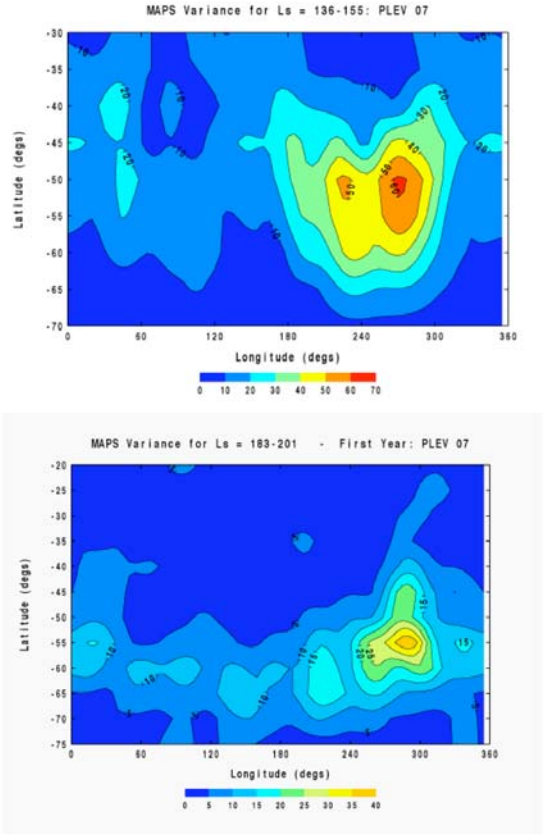

Fig. 2: Storm zone plots at the ~3.7 mb level, obtained via FFSM analyses of the TES temperature data, for two middle and late southern winter periods in the first MGS mapping year.

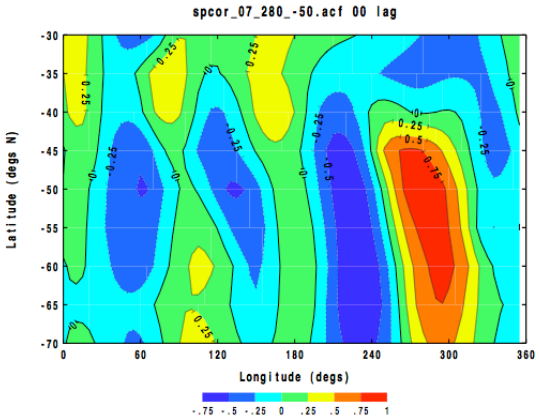

Fig. 3: A single-point eddy correlation map at the 3.7 mb level, computed from TES FFSM products [1], for a mid-winter period in the first mapping year.

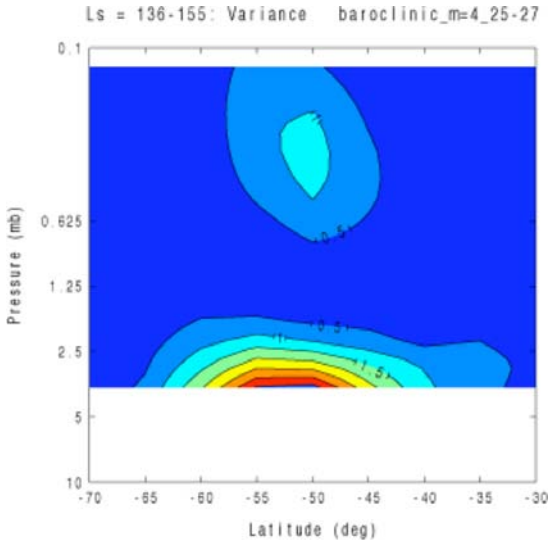

Fig. 4: Amplitude (variance) structure of the dominant wave 4 mode for the L_s~136-155 period in the first mapping year.

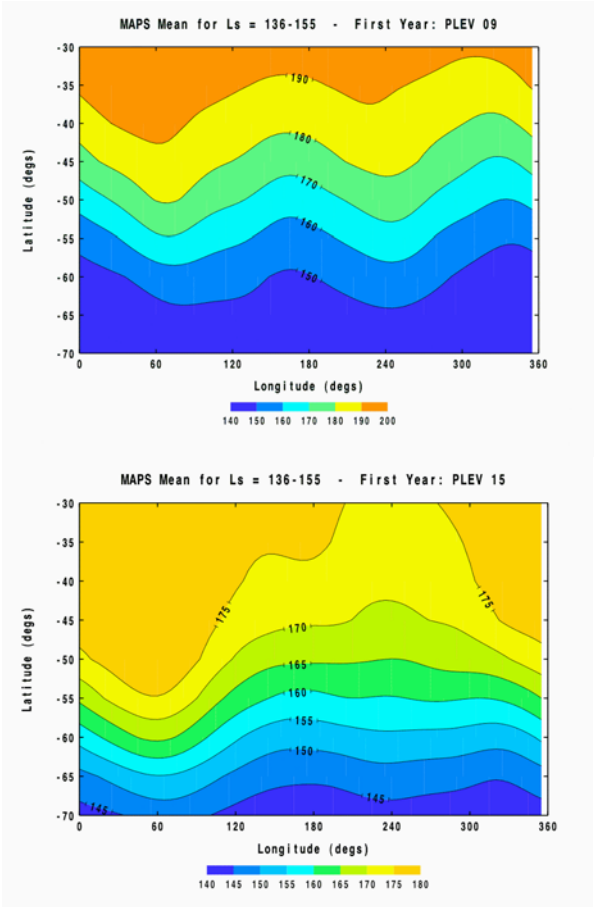

Fig. 5: Time-mean maps of the thermal structure in the TES data at the ~2.2 mb (top) and the ~0.5 mb (bottom) levels, for the L_s~136-155 period in the first mapping year.

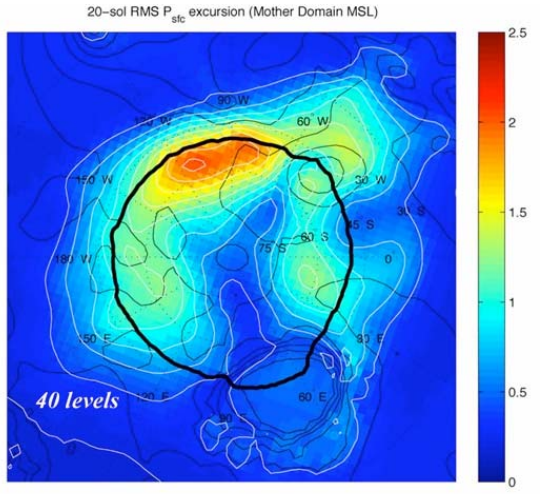

Fig. 6: A storm zone plot for surface pressure from a simulation with the OSU Mars Mesoscale Model for the L_s~120 season in the south. The surface pressure perturbations are normalized to the local mean surface pressure values. The heavy black line is the polar cap edge in the model.

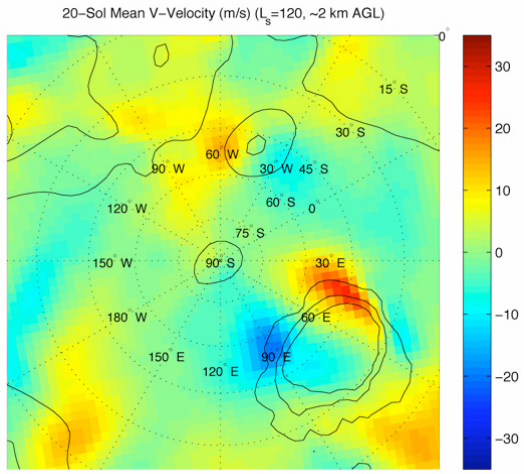

Fig. 7: The time-mean meridional wind field, at about the 2 km level, from the same model simulation as in Fig. 6.